Article
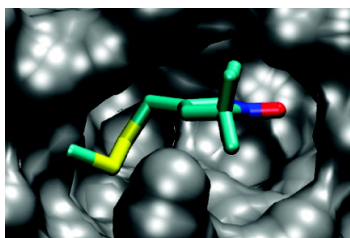
Mapping Electron Paramagnetic Resonance Spin Label Conformations by the Simulated Scaling Method
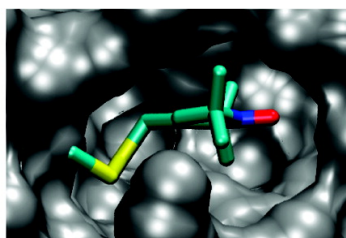
Mikolai I. Fajer, Hongzhi Li, Wei Yang, and Piotr G. Fajer

X-ray Crystal Structure   Simulated Structure

More About This Article

Additional resources and features associated with this article are available within the HTML version:

- Supporting Information
- Links to the 2 articles that cite this article, as of the time of this article download
- Access to high resolution figures
- Links to articles and content related to this article
- Copyright permission to reproduce figures and/or text from this article

View the Full Text HTML

ACS Publications
High quality. High impact.

Mapping Electron Paramagnetic Resonance Spin Label Conformations by the Simulated Scaling Method

Mikolai I. Fajer,[†,#] Hongzhi Li,[⊥] Wei Yang,[†,‖,⊥] and Piotr G. Fajer*,[†,‡,§]

Contribution from the Institute of Molecular Biophysics, Florida State University, Tallahassee, Florida 32306, Department of Biological Sciences, Florida State University, Tallahassee, Florida 32306, National High Magnetic Field Laboratory, 1800 East Paul Dirac Drive, Tallahassee, Florida 32310, Department of Chemistry and Biochemistry, Florida State University, Tallahassee, Florida 32306, and School of Computational Science, Florida State University, Tallahassee, Florida 32306

Received February 27, 2007; E-mail: fajer@magnet.fsu.edu

Abstract: In order to efficiently simulate spin label behavior when attached to the protein backbone we developed a novel approach that enhances local conformational sampling. The simulated scaling (SS) approach (Li, H., et al. *J. Chem. Phys.* **2007**, *126*, 24106) couples the random walk of a potential scaling parameter and molecular dynamics in the framework of hybrid Monte Carlo. This approach allows efficient barrier crossings between conformations. The method retains the thermodynamic detailed balance allowing for determination of relative free energies between various conformations. The accuracy of our method was validated by comparison with the recently resolved X-ray crystal structure of a spin labeled T4 lysozyme in which the spin label was in the interior of the protein. Consistent potentials of mean force (PMF) are obtained for the spin label torsion angles to illustrate their behavior in various protein environments: surface, semiburied, and buried. These PMFs reflect the experimentally observed trends and provide the rationale for the spin label dynamics. We have used this method to compare an implicit and explicit solvent model in spin label modeling. The implicit model, which is computationally faster, was found to be in excellent agreement with the explicit solvent treatment. Based on this collection of results, we believe that the presented approach has great potential in the general strategy of describing the behavior of the spin label using molecular modeling and using this information in the interpretation of EPR measurements in terms of protein conformation and dynamics.

1. Introduction

In recent years, electron paramagnetic resonance (EPR) spectroscopy has been developed as a structural biology method for understanding protein conformation and dynamics. EPR uses extrinsic probes, i.e., spin labels, which are introduced into the targeted regions of a protein. Although this technique has a number of advantages and is complementary to other biophysical approaches, it faces a challenge in interpreting EPR signals that originate from the extrinsic probe in terms of protein conformation and dynamics. This interpretation can only be done if spin label behavior with respect to the protein surface is well characterized. Our approach to predict the spin label behavior is molecular simulations in which spin labels are treated as honorary sidechains.[1-8] Such molecular modeling has proven

to be useful; however it is still technically demanding because molecular simulations are limited by the quasi-ergodicity problem. True ergodicity occurs when the dynamic average of a simulation approaches the thermodynamic average and only occurs when the simulation has sufficiently sampled the conformational space.[9] Ergodicity is tracked by watching the convergence of the dynamic average to a stable result. In some cases, quasi-ergodic solutions are obtained when the dynamic average appears to converge before the conformational space is properly sampled, and in these cases the solutions are representative of a non-canonical ensemble.

In order to resolve this sampling problem in canonical molecular simulations, we previously developed a multistep approach combining Metropolis Monte Carlo Minimization

---

[†] Institute of Molecular Biophysics, Florida State University.
[‡] Department of Biological Sciences, Florida State University.
[§] National High Magnetic Field Laboratory.
[‖] Department of Chemistry and Biochemistry, Florida State University.
[⊥] School of Computational Science, Florida State University.
[#] Current address: Department of Chemistry and Biochemistry, University of California, San Diego, 9500 Gilman Drive MC 0365, La Jolla, CA 92092-0365.

(1) Colombus, L.; Kálai, T.; Jekö, J.; Hideg, K.; Hubbell, W. L. *Biochemistry* **2001**, *40*, 3828−3846.
(2) Hakansson, P.; Westlund, P.; Lindahl, E.; Edholm, O. *Phys. Chem. Chem. Phys.* **2001**, *3*, 5311−5319.
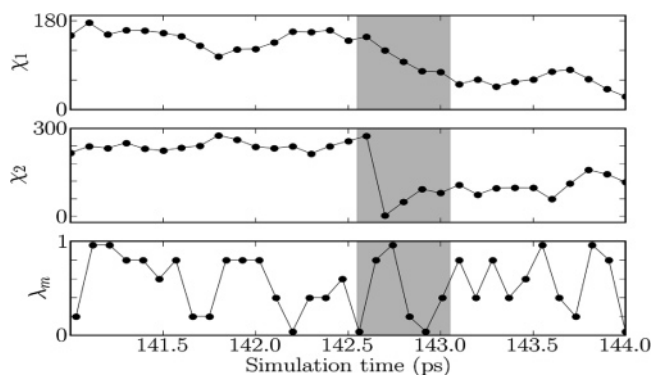(3) LaConte, L. E.; Voelz, V.; Nelson, W.; Enz, M.; Thomas, D. D. *Biophys. J.* **2002**, *83*, 1854−66.
(4) Robinson, B.; Slutsky, L.; Auteri, F. *J. Chem. Phys.* **1992**, *96*, 2609−2616.
(5) Sale, K.; Sar, C.; Sharp, K. A.; Hideg, K.; Fajer, P. G. *J. Magn. Reson.* **2002**, *156*, 104−12.
(6) Steinhoff, H. J.; Hubbell, W. L. *Biophys. J.* **1996**, *71*, 2201−12.
(7) Steinhoff, H.-J.; Müller, M.; Beier, C.; Pfeiffer, M. *J. Mol. Liq.* **2000**, *84*, 12−27.
(8) Timofeev, V. P.; Nikolsky, D. O. *J. Biomol. Struct. Dyn.* **2003**, *21*, 367−78.
(9) Becker, O. M.; Watanabe, M. In *Computational Biochemistry and Biophysics*; Becker, O. M., MacKerell, A. D., Jr., Roux, B., Watanabe, M., Eds.; Marcel Dekker, Inc.: 2001; pp 39−69.

(MMCM) with molecular dynamics (MD) simulations.[10,11] First, an MMCM search is applied to exhaustively locate low energy conformers in the spin label dihedral space while keeping the rest of the protein structure rigid (*rigid cage* assumption). MD simulations are then used to sample the local environment of the MMCM low energy conformers with the *rigid cage* assumption relaxed. It is noted that the *rigid cage* assumption used in the first step biases the conformational search toward the initial structure of a protein.

Although multiple energy wells are sampled in MMCM/MD, it is difficult to determine the relative weights between the populations of various conformers, which are separately simulated in the MD step. With this concern in mind, we adopt a recently developed simulated scaling (SS) method[12] that interleaves the elements of MC and MD into single simulations so as to preserve the thermodynamic detailed balance among various conformers, in particular the conformers separated by nontrivial barriers. The SS method is a potential scaling version of the simulated tempering technique which utilizes a *generalized ensemble* with a modified Wang−Landau updating scheme to ensure an efficient random walk of the scaling parameter.[13]

In the present work, we demonstrate that this advanced sampling method can be used to efficiently and quantitatively map spin label conformations. We have applied this method to the commonly used methanethiosulfonate spin label (MTSSL) in various protein environments: (*i*) on a protein surface, where motion, in the absence of any steric constraints, is dominated by the rotations around the distal (fourth and fifth) bonds of the spin label (referred to as the $\chi 4/\chi 5$ motional model); (*ii*) as a semiburied residue with some steric restrictions; (*iii*) and a buried residue, in which the steric constraints exclusively determine the label conformation. Crystal structures of spin labeled *T4 lysozyme* were chosen to represent the protein surface and buried environments (pdb 2cuu [Fleissner and Hubbell to be published] and pdb 2nth,[14] respectively). A computationally mutated *Staph.* nuclease (pdb 1ey0[15]) was selected for the semiburied environment. We have obtained consistent descriptions of spin label conformational maps in various protein environments and excellent agreement between simulated conformation and recently resolved crystal structure. In addition, the similarity of the torsional potential of mean force (PMF) using an explicit solvation model (TIP3P) and a simple implicit solvent treatment (distance dependent dielectric constant, or DDE) validates the usage of the implicit solvent, which is computationally more efficient, without sacrificing the conformational accuracy.

Thus, we believe that application of the SS method to map EPR spin label conformations can strengthen the promise of the general strategy in combining EPR measurement and simulated data to understand protein conformation and dynamics.

(10) Sale, K.; Song, L.; Liu, Y. S.; Perozo, E.; Fajer, P. *J. Am. Chem. Soc.* **2005**, *127*, 9334−5.
(11) Fajer, P. G.; Gyimesi, M.; Málnási-Csizmadia, A.; Bagshaw, C. R.; Sen, K. I.; Song, L. *J. Phys.: Condens. Matter* **2007**, *19*, 285208.
(12) Li, H.; Fajer, M.; Yang, W. *J. Chem. Phys.* **2007**, *126*, 024106.
(13) Wang, F.; Landau, D. P. *Phys. Rev. Lett.* **2001**, *86*, 2050−3.
(14) Guo, Z.; Cascio, D.; Hideg, K.; Kalai, T.; Hubbell, W. L. *Protein Sci.* **2007**, *16*, 1069−86.
(15) Chen, J.; Lu, Z.; Sakon, J.; Stites, W. E. *J. Mol. Biol.* **2000**, *303*, 125−30.

Figure 1. Dihedrals $\chi 1$, $\chi 2$, and the λ scaling factor during an SS simulation. For definition of $\chi 1$ and $\chi 2$ dihedrals, see Figure 2.

2. Theory and Methods

2.1. Simulated Scaling Method. The SS method was introduced by Yang[12] and is detailed in the Supporting Information. Briefly, the method represents a system with the potential $U_o = U_s + U_e$, where U_s are the energy terms determining the local conformations in the region of interest (for instance, spin label residues), and U_e is the collection of environmental energy terms. In the scaled simulations we construct an expanded ensemble with one additional dimension represented by λ_m, and the energy potential is generalized as in eq 1:

$$U = \lambda_m U_s + U_e \tag{1}$$

A random walk in λ_m space facilitates energy barrier crossing. For $\lambda_m < 1$, the potential energy barriers are lowered, and barrier crossing occurs more frequently. The return of λ_m to 1 allows the sampling of a new conformation with the original potential. Only the torsional and nonbonded energy terms are included in U_s.

To illustrate the barrier crossing mechanism, a transition event in an SS simulation of MTSSL is shown in Figure 1. Prior to the highlighted region $\chi 2$ is in a stable conformation at 240°. In the highlighted region, λ_m is at 0.04 and the potential energy barrier at $\chi 2 \approx 150°$ has been reduced to essentially zero. A sharp transition of $\chi 2$ follows and λ_m increases, restoring the potential barrier. $\chi 1$ adopts a new value of ∼60° during the next occurrence of a low potential, resulting in a stable conformation that is then sampled.
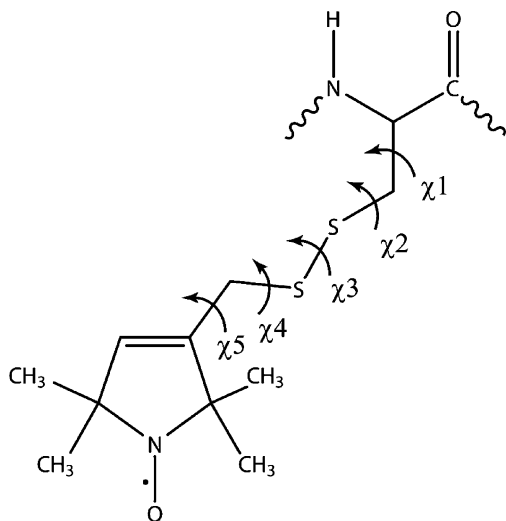
2.2. Data Analysis. In order to quantitatively analyze spin label conformations, the potential of mean forces (PMF, symbol W) is computed around pairs of adjacent dihedral angles as in eq 2,

$$W(\chi 1, \chi 2) = -RT \ln(\rho(\chi 1, \chi 2)) + C \tag{2}$$

where $\rho(\chi 1, \chi 2)$ represents the occurrence probability at $(\chi 1, \chi 2)$ from the samples with a full potential. For the calculation of the occurrence probabilities, each two-dimensional conformation space is divided by a number of rectangle bins with $10° \times 10°$ as one binning unit. The upper limit of observable energies is imposed by the simulation temperature and time scale. In our simulations the upper limit of sampled energies within a conformation is 4 kcal/mol. This means that all the transition barriers lower than 4 kcal/mol are correctly determined, but transition barriers greater than 4 kcal/mol are undetermined.

2.3. Molecular Modeling. In order to characterize only the spin label motion in the local environment all atoms beyond a 15 Å sphere centered on the spin label were restrained. The protein backbone was also restrained. The V131C mutation of *T4 lysozyme* (pdb 2cuu) was selected to examine spin label motion in a protein surface environment. The T118C mutation of *T4 lysozyme* (pdb 2nth) was selected for a protein interior, or buried environment. Finally the M65C mutation in *Staph.* nuclease wild type (pdb 1ey0) offered a semiburied environment. In the case of the M65C system the native methionine residue was

Figure 2. MTSSL spin label consists of a five-member nitroxide ring attached via a tether to the protein backbone. The conformation of the spin label is defined by the five torsional angles $\chi 1 - \chi 5$. Torsional angles are considered to be zero when eclipsed and right-handed motion is taken to be positive. The following definition will also be used: gauche+ (60°), trans (180°), and gauche− (300°).

"mutated" to MTSSL (Figure 2) using a PSFGEN script.[16] The crystal structures of the spin labeled mutants V131C and T118C were used, although the initial conformation of the spin label was randomized prior to simulation.

The Metropolis Monte Carlo Minimization searches of spin labels were originally described in Sale et al.[5] and are reviewed in the Supporting Information. The simulations were performed with the CHARMM19 and CHARMM27 force fields for the implicit solvent (distance dependent dielectric solvation method) and for the explicit solvent model (TIP3P), respectively. The four lowest energy MMCM structures were used as the initial structures for the MD and SS simulations. Again, the details are in the Supporting Information.

The simulation convergence was monitored by calculating the PMFs at different simulation times. The MD simulations converged for all the local minima after 0.5−1.0 ns. The SS simulations took longer to converge due to the larger conformational space searched and was on the order of 10−20 ns to achieve proper convergence.

3. Results

3.1. Conformational Sampling Using the MMCM/MD and the SS Methods. The four lowest energy rotamers of the *Staph.* nuclease M65C mutant were identified by MMCM searches (Figure 3A′−D′). These rotamers were used as the initial structures for subsequent MD simulations. The resulting PMF corresponding to the MTSSL's $\chi 1/\chi 2$ dihedral space (Figure 3A−D) reveals at least three distinct $\chi 1/\chi 2$ conformers: I = (189° ± 15°, 95° ± 20°); II = (315° ± 15°, 293° ± 25°), and III = (305° ± 10°, 115° ± 25°). These conformations agree with the consensus torsion angle minima for $\chi 1$ (60°, 180°, 300°).[17] Although, the minimum values are in good agreement, MD has a problem with sampling the transitions between the minima. In our MD simulations the spin label is caught within one or two local minima, confirming that the classical MD simulation should not be used for conformational searching.

The two-stage hybrid MMCM/MD approach has two drawbacks: (1) To make the MMCM method computationally

(16) Fajer, M.; Sale, K.; Fajer, P. In *ESR Spectroscopy in Membrance Biophysics*; Berliner, M. H. a. L., Ed.; Springer-Verlag: 2007; pp 253−259.
(17) Brooks, B. R.; Bruccoleri, R. E.; Olafson, B. D.; States, D. J.; Swaminathan, S.; Karplus, M. *J. Comput. Chem.* **1983**, *4*, 187−217.

feasible, the protein atoms are fixed and only the spin label atoms are allowed to move, the so-called *rigid cage* assumption. The energy ranking obtained from the first stage can only roughly represent the energetics of the protein environment where all atoms are allowed to move. The energy-ranking among the lowest energy conformers can rearrange after the whole system is relaxed. Such a rearrangement was observed after simulated annealing in some cases. Hence, the *rigid cage* assumption in the MMCM method makes the choice of initial structures for MD somewhat arbitrary. (2) The other problem with the MMCM/MD approach is that separate PMFs generated in the MD step cannot be easily merged. A common reference conformation is required for such merging, and there is little to no conformational overlap of all atoms from different MD trajectories. This lack of ease in merging trajectories results in the loss of the relative weighting of minima from different PMFs.

As described in the theory section, the simulated scaling method circumvents these two problems by integrating an exhaustive searching component (MC) and a local conformational sampling component (MD) into a single simulation. The same four distinct rotamers used in the previous MD simulations (Figure 3) were used for four SS simulations. The potentials of mean force from these 2 ns SS simulations are shown in Figure 4. The most striking feature is that they yielded identical results independent of the initial structures, implying that the SS simulations exhaustively sampled the available conformational space and converged on the same conformations.

SS simulations resolve the quasi-ergodicity problem of the MD simulations. The transition between region I and II in Figure 4 that was difficult in MD proceeds readily since the two torsion potential barriers are reduced. Within each of these four simulations, conformational transitions among the different minimum regions occurred frequently enough to ensure the convergence of each trajectory. The PMF minima observed in the SS trajectories correspond to the MMCM/MD minima. The selection of initial structures is no longer an issue because the SS simulations sample all of the available conformers within a single nanosecond-scale trajectory and provide the relative weighting of the conformers. Furthermore, the simulations are performed without a *rigid cage* assumption, and thus the PMF differences correspond to differences in the free energy of the conformers including their dynamic protein environment.

The convergence of the SS simulations for the $\chi 1/\chi 2$ dihedral space in Figure 4 extends to the entire dihedral space of the spin label, Figure 5. As before the potential of mean force for the distal bonds is identical for each of the four conformers (at a contour level of 2 kcal/mol).
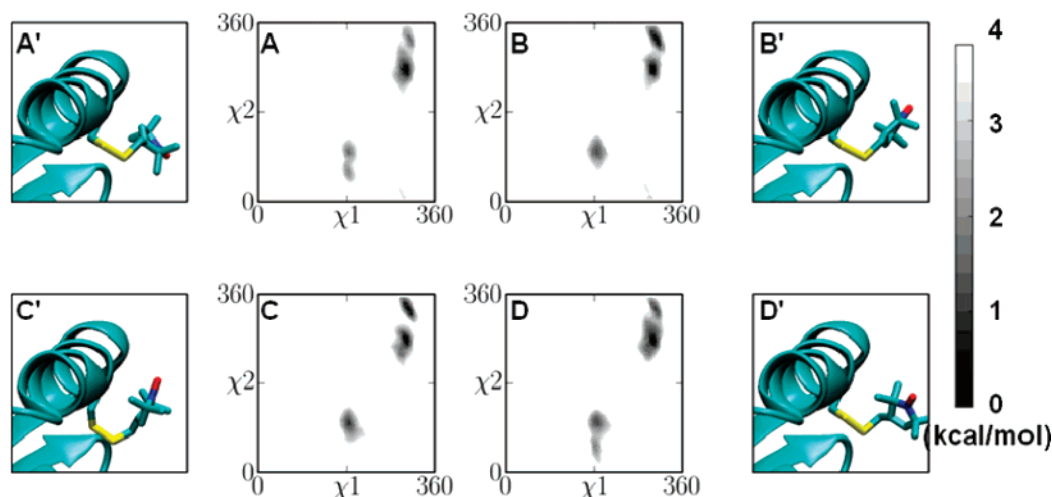
3.2. Solvent Model: Implicit and Explicit Water. The efficient sampling of the SS method facilitated comparison of two commonly used solvent models: distance dependent dielectric (DDE, an implicit solvent treatment) and the TIP3P (an explicit solvent treatment). The former is computationally more efficient (5−10 times faster), but its ability to accurately model spin label conformations had to be ascertained. We compared the two solvent models using both MMCM/MD and SS methods on the MTSSL conformational space of *Staph.* nuclease M65C, all simulations beginning with the same initial conformation.
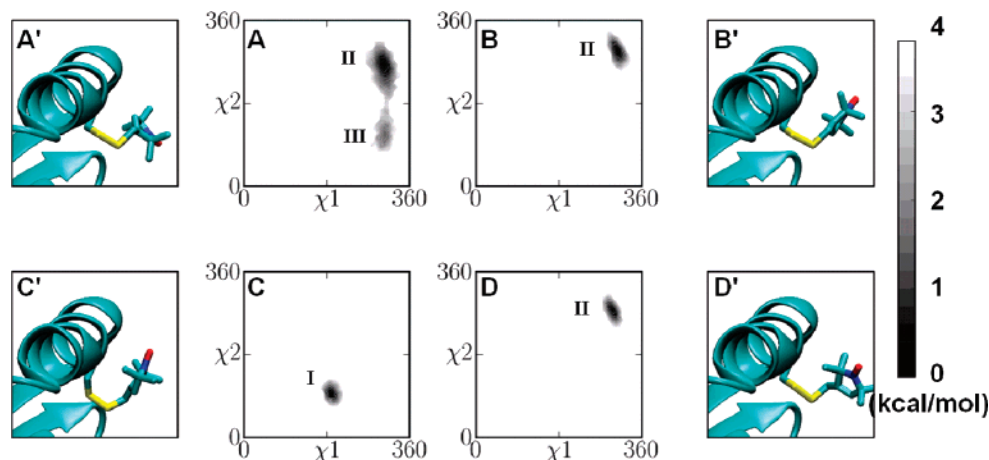
Figure 3. Potential of mean force in the dihedral space ($\chi 1-\chi 2$) occupied by MTSSL spin label on site 65 of *Staph.* nuclease. Panels (A–D) represent the results of MD simulations from different initial conformations shown in panels (A′–D′).
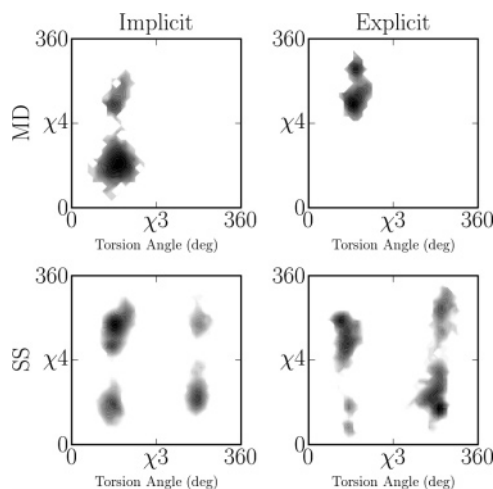

Figure 4. Potential of mean force in the dihedral space ($\chi 1-\chi 2$) occupied by MTSSL spin label on site 65 of *Staph.* nuclease. Panels (A–D) represent the results of SS simulations from different seed conformations in panels (A′–D′).
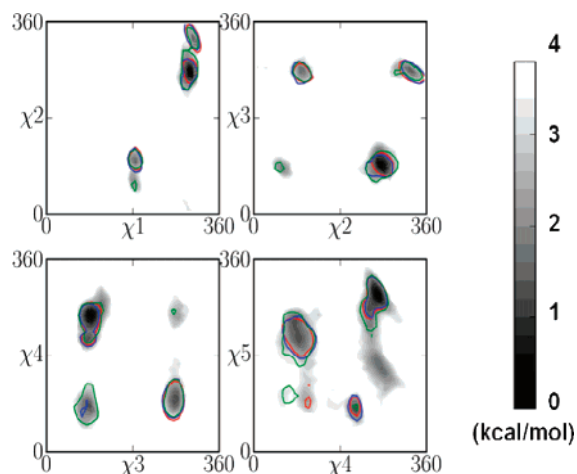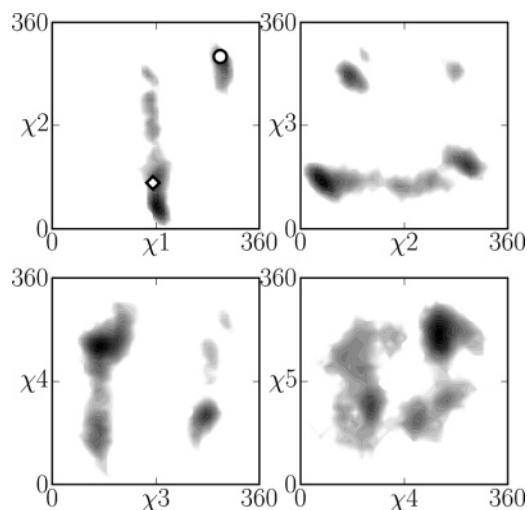

Figure 5. Potential of mean force in the complete dihedral space occupied by MTSSL spin label on site 65 of *Staph.* nuclease. The grayscale filled contour shows the result of the A simulation. The red, green, and blue are the B, C, and D SS simulations, respectively, drawn at a contour level of 2 kcal/mol.

Figure 6. Comparison of the $\chi 3/\chi 4$ dihedral space for different sampling techniques and different solvent models using the M65C initial structure from Figure 4A. *Top*: comparison of the DDE and TIP3P solvent model for the MMCM/MD technique. *Bottom*: comparison of the solvent models for the SS technique.

In general the starting conformation was the only one populated in the MD simulations, irrespective of the solvent model. The results illustrated in Figure 6 represent the worst case scenario, with considerable dependence on the solvent

model in the MD simulations but not for the SS simulations. The time series of $\chi 4$ for the DDE MD shows that the spin label side chain begins with a $\chi 4$ of approximately 235° (region

Figure 7. Potential of mean force in the dihedral space occupied by MTSSL spin label on site V131 of T4 lysozyme. The resolved X-ray crystal conformers A and B are shown as the diamond and circle, respectively.

I) and undergoes a transition to 90° (region II). However, when the explicit solvent model was used, a different transition occurs, ending with a χ4 of 300° (region III). It seems unlikely that the difference is due to the different solvent models. The difference could be due to differences in sampling efficiency, i.e., the inability of MD to efficiently transition between conformers. On the other hand, the SS simulations show no difference between solvent models. This example illustrates the importance of exhaustive sampling when comparing simulation methods and parameters.

3.3. Protein Environment − Surface, Semiburied, and Buried Residues.

3.3.1. Surface Residue. The T4 lysozyme mutant V131C is a surface residue and as such does not experience strong steric restrictions. The X-ray structure for the MTSSL mutant has been recently solved by Fleissner and Hubbell (pdb # 2CUU). The X-ray electron density of the MTSSL was well resolved up to the SG, and thus the χ1 and χ2 torsion angles are well-defined. The X-ray values for the dihedrals overlaid on the SS results (Figure 7) show excellent agreement for the simulated and experimentally resolved dihedrals. The simulations show a progression of flexibility down the length of the spin label; i.e., the angular spread of the occupied conformational regions is in the order χ4/χ5 > χ3/χ4 > χ2/χ3 > χ1/χ2. The χ1 closely follows the canonical values of *gauche−* and *trans* conformations, but the *gauche+* is missing. The V131 position is not an ideal surface residue due to large adjacent side chains (D127, E128, and K135) that interfere with the χ1 *gauche+* conformation. The χ3 dihedral has two distinct minima , and the χ4 and χ5 values exhibit little preference in agreement with the large dynamics of these dihedrals ("χ4/χ5" model) proposed from the observed EPR mobility of the MTSSL label.[1]

3.3.2. Semiburied Residue. The *Staph.* nuclease M65C mutant shown in Figure 5 is a semiburied residue, in proximity to the 99−106 helix, 93−98 loop, and 69−72 loop. The χ1 torsion angle takes two canonical values of *trans* and *gauche−*, and the χ2 angle also has a limited distribution. The *gauche+* χ1 conformer is not accessible due to the α-helical secondary structure. The disulfide bond (χ3) corresponds to the canonical values of 90° and 250°. Broad distributions of the χ4 and χ5

Table 1. . Dihedral Values for the Best Conformers of MTSSL at T118C of T4 Lysozyme

| dihedral angle	X-ray	simulation scaling (initial structure)			
		SS1	SS2	SS3	SS4
χ1	256°	246°	213°	309°	316°
χ2	33°	27°	133°	238°	318°
χ3	88°	85°	273°	109°	265°
χ4	54°	45°	146°	84°	282°
χ5	107°	113°	210°	232°	275°

angles indicate that they are free of any steric collision, as the length of the spin label tether brings the nitroxide ring above the surface of the other side chains, and the distal part of the label behaves is free to move as observed for the surface residues.

3.3.3. Buried Residue. An excellent example of the buried residue is the T4 lysozyme mutant T118C modified with the MTSSL, whose X-ray structure has also been recently solved by Fleissner and Hubbell and made available prior to publication. Since the electron density for all the MTSSL atoms is resolved in the X-ray structure, the predictive power of the SS method can be validated. The label at the T118 position makes tertiary contacts with both helix 82−90 and loop 107−114. The SS simulation yields four distinct minima (referred to as SS1−SS4, tabulated in Table 1). The minimum SS1 is the same conformation observed in the crystal structure.

Visual inspection of the labeled T118C site (Figure 8) shows that the protein cavity is only slightly larger than the size of the spin label, and all four minima fit snugly into this cavity. During the SS simulation, transitions between minimum energy conformations only occurred for greatly reduced conformational barriers ($\lambda_m \leq 0.6$) and involved correlated dihedral rotations (data not shown).

It is worth noting that steric restrictions of the buried site override the "χ4/χ5" model. The distal bonds have well-defined values and display little variation caused by the tight packing around the nitroxide methyl groups, visualized in Figure 8, which limits the label's motional freedom.
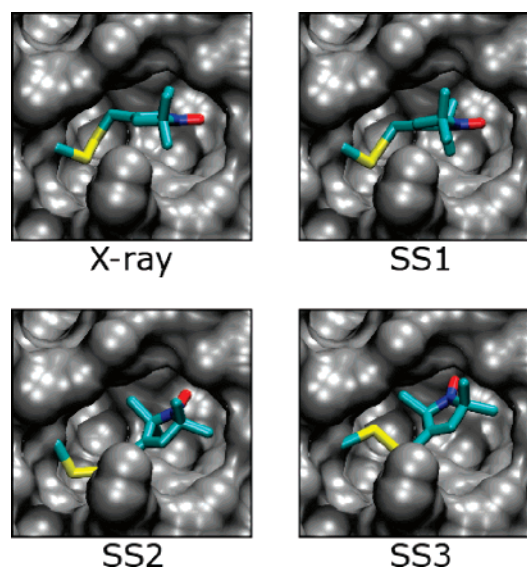
Figure 8. Visualization of the T118C site of T4 lysozyme. The protein backbone and sidechains are shown in a surface representation, and the MTSSL spin label is shown as sticks.

4. Discussion

The comparison of the spin label conformational potentials of mean force, generated in simulations with different initial structures, showed that the simulated scaling technique is exhaustive in searching the conformational space of the spin label in the dynamic protein environment. The comparison of two widely used solvent models, distance dependent dielectric (implicit) and TIP3P (explicit), revealed no significant difference in the range of label conformations justifying the use of a simpler and computationally faster solvent model. The method was validated with X-ray structures of spin labeled T4 lysozyme. Simulated scaling simulations of the surface residue V131C and the buried residue T118C of T4 lysozyme correctly identified the X-ray crystal structure conformations.

The efficiency of the SS method in sampling the conformational space is attributed to interleaving the elements of molecular dynamics and Monte Carlo within a single trajectory. As in MMCM the random MC steps of SS allow conformational searching when the potential energy barriers limit direct transition between conformations. The SS methods also allow for the dynamic nature of the protein environment. The spin label diffusion occurs in the MD-like, fluid environment, where protein sidechains and backbone are allowed to respond to the motion of the spin label.

The quasi-ergodicity limitations of MD and MC are well-known, and long nanosecond simulations are not a guaranteed solution.[18] The g*eneralized ensemble* methods, of which SS is a member, allow a free random walk instead of a Boltzmann weighted random walk in the potential energy space.[19] A free random walk is able to search the space more exhaustively and efficiently. The advantage of SS over the other *generalized ensemble* methods such as simulated tempering and replica exchange is in the limitation of the degrees of freedom. A flat potential ($\lambda_m = 0$ for one of the replicas) is the equivalent of infinite temperature in the simulated tempering and replica exchange methods; however in the two latter cases use of infinite temperature would result in simulation instability. SS is stable since it limits this "infinite temperature" regime to a small region, and then only to the torsional and nonbonding energy terms. The size of the sampling region is a tradeoff for the SS efficiency. SS provides efficient sampling of a small region, whereas the other *generalized ensemble methods* have a larger sample region, but are less efficient. Details of SS simulations and a list of other applications outside of exhaustive conformational searching can be found in ref 12.

The ergodicity (exhaustiveness) of any computational simulation is a prerequisite for accurate modeling of molecular behavior. For instance, the limited sampling of the MMCM/MD would suggest a difference between the solvent models, Figure 6, which vanished with the proper conformational sampling provided by SS. The exhaustive sampling and the dynamic environment allow simulations of spin label behavior in a more accurate physical model. In addition, the ergodicity of a single simulation allows for an internal reference of free energy. This, in turn, facilitates determination of the relative populations of different conformers in solution. This point can be validated by decomposition of EPR spectra into components

corresponding to a single conformer, which is the focus of future work. To freeze the exchange between conformer populations high-frequency EPR may be needed. Multiple conformer populations contributing to EPR spectra have been observed in the past.[1,20,21] The EPR spectra of such conformational populations have been simulated from molecular modeling,[22] and the relative weights of the simulated EPR spectra can be determined from SS and compared to experiment.

The thermodynamic balance of various conformers is needed in the characterization of protein folding or enzymatic reactions. The spectral components were previously assumed to correspond to different protein states. The molecular modeling presented here helps identify the number of distinct spin label conformations for a specific protein state and labeled site. This information is a prerequisite to the identification of which spectral components correspond to distinct spin label states of a specific protein conformation and which components correspond to a distinct protein conformation. Too often we do not make this distinction and ascribe the spectral components to unique protein conformations. The changes of the spectral components corresponding to the label conformations with temperature can be accounted for by the thermodynamic balance from SS simulations, which then yield thermodynamic information about the different protein conformations.

The distance dependent dielectric implicit solvent model is a compromise between the efficiency of a vacuum model and accuracy of an explicit solvent model. During parametrization the models are tested on simple cases to reproduce macroscopic parameters like pressure, dielectric constant, etc. Our comparison between DDE and TIP3P solvent models dealt only with the comparison of local conformational distributions of a labeled side chain, which was independent of a solvent model. In this context, the implicit solvent treatment provides a significant gain of computational speed over the explicit solvent without sacrificing the accuracy.

Past comparisons between solvent models have shown varying degrees of agreement.[23-25] Comparisons often involve quantities such as RMSD, RMSF, and torsional populations or free energies. These quantities are all susceptible to improper sampling. Of particular interest is an MD study of the side chain torsional angles in the Met-enkephalin peptide.[25] A TIP3P, atomic solvation parameter, solvent-accessible surface area, and vacuum solvent model were compared and yielded significantly different distributions of $g+$, t, and $g-$ for $\chi 1$ of Tyr and Phe. The current work suggests that the differences previously observed in solvent comparisons were possibly due to the quasi-ergodicity problem as shown in Figure 6, which can be overcome with *generalized ensemble* methods.

The SS method passed a validation test against two crystal structures of a spin labeled protein. In the structure for the buried residue the spin label electron density is very well resolved including the center of the nitroxide ring (Hubbell, W. Private

(18) Caves, L. S. D.; Evanseck, J. D.; Karplus, M. *Protein Sci.* **1998**, *7*, 649–666.

(19) Okamoto, Y. *J. Mol. Graphics Modell.* **2004**, *22*, 425–39.

(20) Barnes, J. P.; Liang, Z.; McHaourab, H. S.; Freed, J. H.; Hubbell, W. L. *Biophys. J.* **1999**, *76*, 3298–306.

(21) Langen, R.; Oh, K. J.; Casicio, D.; Hubbell, W. *Biochemistry* **2000**, *39*, 8396–8405.

(22) Budil, D. E.; Sale, K. L.; Khairy, K. A.; Fajer, P. G. *J. Phys. Chem. A* **2006**, *110*, 3703–13.

(23) Arnold, G. E.; Ornstein, R. L. *Proteins: Struct., Funct., Genet.* **1994**, *18*, 19–33.

(24) Feig, M.; Chocholousova, J.; Tanizaki, S. *Theor. Chem. Acc.* **2006**, *116*, 194–205.

(25) Shen, M. Y.; Freed, K. F. *Biophys. J.* **2002**, *82*, 1791–1808.

communication). The SS predicted four conformations, Table 1. These conformations were not "connected"; i.e., to transit from one conformation to another requires correlated rotation about multiple bonds. The free energy barrier and path for these transitions were not determined but were only observed for low λ_m values and are expected to be quite high. One of these conformations (SS1, Table 1) is within several degrees of the crystal structure on all dihedral angles. The other two conformations are not observed in the crystal, but this can be rationalized as the static molecular structures in a crystal rarely reflect thermodynamic equilibrium in an aqueous solution. An alternative explanation is that protein folding predisposes one possible conformer over the other, and the large energy barriers between conformational transitions result in a kinetically trapped local minimum. The crystal structure of the surface residue was also well reproduced by SS simulation (Figure 7) for the atoms resolved in the crystal structure. The atoms for which there was no electron density imply large conformational disorder, which was observed in our simulations. Similar test validations were performed previously;[5] however this is the first direct comparison to the crystal structure of a spin label bound to the protein. The previous efforts involved EPR and electron microscopy both of which have lower resolution than that of X-ray, and the sample was ordered in 1D (oriented muscle fiber) as opposed to a 3D crystal here. Our agreement with the crystal structures gives us confidence in our ability to predict the orientation of the spin labels in tertiary contacts.

In the case of surface residues the proximal bond dihedrals, $\chi1 - \chi3$, take on canonical values in the SS simulations. Our force fields are not parametrized for the presence of the possible hydrogen bond between $C_\beta-H$ and S_δ, the presence of which would bias the energetics and geometry of these dihedrals. This does not seem to be an overwhelming problem, because for the surface residues the mobility of $\chi4$ and $\chi5$ dominates label dynamics. Furthermore, the preliminary work predicting the orienting potentials for label motion showed good agreement using the current force field and observed EPR spectra.[22] For the semiburied and buried residues it is the steric contacts that define the conformational energetics. These restrictions are primarily on the proximal angles $\chi1/\chi2$, and for geometrical reasons the angles near the protein backbone will influence most the position of the nitroxide ring. As we move away from the backbone, the influence of steric interactions from adjacent side chains is reduced and in some cases the range of $\chi4/\chi5$ is again unrestricted, Figure 5. The dependence of the results on the torsion force field parameters was checked and using the parameters derived from the CHARMM27 force field instead of those from the CHARMM19 force field in conjunction with the implicit solvent model had little effect on the derived potentials of mean force (data not shown).

In summary, we have developed a novel approach for prediction of spin label behavior on a protein by employing the simulated scaling method. The method is exhaustive within a single simulation allowing correct energy referencing between conformations. The label conformation distributions were independent of the solvent model affording fast and efficient simulations with an implicit solvent model. The experimental trends in the label mobility for surface and semiburied residues were reproduced in the simulations. Importantly, the method predicted accurately the conformation of a surface and a buried residue as observed in the crystal structures of a labeled protein.

Note Added after ASAP Publication. Due to a production error, the images for Figures 6 and 7 were reversed in the version of this paper published ASAP October 19, 2007. The corrected version was published ASAP October 23, 2007.

Supporting Information Available: A detailed description of the Simulated Scaling method and the simulation details. This material is available free of charge via the Internet at http://pubs.acs.org.

JA071404V